MicroRNA expression profiles in rats with selenium deficiency and the possible role of the Wnt/β-catenin signaling pathway in cardiac dysfunction

YUJIE XING[1], ZHONGWEI LIU[1], GUANG YANG[1,2], DENGFENG GAO[1] and XIAOLIN NIU[1]

[1]Department of Cardiology, The Second Affiliated Hospital, Xi'an Jiaotong University School of Medicine, Xi'an, Shaanxi 710004; [2]Department of Cardiology, Shaanxi Province People's Hospital, Xi'an, Shaanxi 710068, P.R. China

Abstract. Selenium deficiency is a causative factor in heart failure and microRNAs (known as miRNAs or miRs) play an important role in numerous cardiovascular diseases. However, the changes of miRNA expression during selenium deficiency and whether selenium deficiency is involved in cardiac dysfunction remain unclear. In the present study, miRNA expression profiling was carried out in normal rats, selenium-deficient rats and selenium-supplemented rats by miRNA microarray. Cardiac function was evaluated by analyzing the plasma brain natriuretic peptide level, echocardiographic parameters and hemodynamic parameters. Cardiac glutathione peroxidase activity was assessed by spectrophotometry. The histological changes were examined by hematoxylin and eosin staining. Electrocardiograph was used to test the arrhythmia. The differentially expressed miRNAs were verified by reverse transcription-polymerase chain reaction. Additionally, the underlying mechanism associated with the Wnt/β-catenin signaling pathway was further explored. The cardiac dysfunction of the rat with selenium deficiency was mainly associated with five upregulated miRNAs, which were *miR-374, miR-16, miR-199a-5p, miR-195* and *miR-30e**, and three downregulated miRNAs, which were *miR-3571, miR-675* and *miR-450a**. Among these, the expression of *miR-374* was the highest, which may be of vital importance in rats with selenium deficiency. In conclusion, the possible mechanism of selenium deficiency-induced cardiac dysfunction was associated with the Wnt/β-catenin signaling pathway.

Correspondence to: Professor Xiaolin Niu or Professor Dengfeng Gao, Department of Cardiology, The Second Affiliated Hospital, Xi'an Jiaotong University School of Medicine, West Five Road 157, Xi'an, Shaanxi 710004, P.R. China
E-mail: niuxiaolin1@163.com
E-mail: gaomedic@163.com

Introduction

Selenium deficiency is considered a causative factor in various types of heart failure, including Keshan disease (KD), which is prevalent in China and is also one of the most harmful endemic diseases (1). Heart failure patients with reduced left ventricular contractility or systolic heart failure have lower blood selenium levels (2-4). In a small clinical study, selenium improved left ventricular function and quality of life in systolic heart failure (5). However, the selenium deficiency and cardiac dysfunction link remains to be understood.

microRNAs (miRNAs or miRs) are a class of endogenous non-coding small RNAs that are involved in the modulation of numerous biological processes by base-pairing, usually imperfectly, to the 3' untranslated region of a target mRNA, leading to post-transcriptional inhibition and occasionally mRNA cleavage (6). miRNAs have been identified in the majority of types of cells and tissues. The current estimate is that 10-30% of genes may be regulated by miRNAs, particularly the members of signal transduction networks. Additionally, there is increasing evidence that miRNAs are involved in a numerous biological processes, including cell proliferation, differentiation, apoptosis and tumorigenesis (7). Aberrant and/or absent miRNA expression is frequently associated with pathophysiological disorders (8-10). However, miRNA expression changes in the condition of selenium deficiency and whether selenium deficiency is involved in cardiac dysfunction remains unclear.

Wnt/β-catenin signaling is subjected to multiple levels of molecular control. The canonical Wnt/β-catenin signaling pathway is initiated when Wnt ligands bind to its receptor(s), Frizzled (11) and low-density lipoprotein receptor-related protein-5 or -6 (LRP5 or LRP6) (12). The stabilized β-catenin accumulates in the cytoplasm and translocates into the cell nucleus following activation, where it forms a β-catenin-lymphoid enhancer-binding factor (LEF)/transcription factor (TCF) transcriptional complex and induces transcription of downstream genes implicated in carcinogenesis. In the absence of Wnt-ligand stimulation, β-catenin is sequestered in the 'destruction complex,' which leads to β-catenin degradation by the ubiquitin-proteasome mechanism and ultimately the inactivation of β-catenin signaling (13-15).

The secretion of antagonists of the Wnt pathway, including Wnt inhibitory factor-1, secreted Frizzled-related proteins and Dickkopf1 (16) also regulate the suppression of β-catenin signaling. Wnt proteins belong to a large family of cysteine-rich secreted glycoproteins, which are highly conserved during evolution, and they activate a highly conserved intracellular signaling cascade with a significant influence in early embryogenesis and pattern regulations (17,18). These proteins have diverse mediated effects, including proliferation, apoptosis, migration, polarization, stem cell maintenance and differentiation (19). Wnt/β-catenin signaling plays significant roles in animal development and tissue homeostasis, and misregulation of this pathway has been associated in numerous pathological states, such as cancer, heart disease and Alzheimer's (20).

Given the potential role of miRNAs, their expression was profiled in selenium-deficient rats by microarray. The differentially expressed miRNAs were selected and validated. Due to the importance of Wnt/β-catenin signaling in cardiac function, it was further investigated in an attempt to provide a novel insight into the limited understanding of the biological process and mechanism of cardiac dysfunction in selenium-deficient rats.

Materials and methods

Animals. A total of 60 male weaning Sprague-Dawley rats (3-weeks old; specific-pathogen-free class; body weight, 75±10 g) were raised under controlled-environmental conditions (12-h light-dark cycle; temperature, 25±1˚C; humidity, 65±4%). The standard diet (containing 0.2 mg selenium/kg food) was produced by the Animal Experimental Center of Xi'an Jiaotong University (Xi'an, China) and the low-selenium diet (<0.02 mg selenium/kg food) was produced by Trophic Animal Feed High-tech Co. (Jiangsu, China) according to the AIN-93 M formula. The food was stored at 4˚C and fresh tap water was allocated continuously. The study was carried out in strict accordance with the recommendations in the Guide for the Care and Use of Laboratory Animals of the National Institutes of Health. The protocol was approved by the Committee on the Ethics of Animal Experiments of Xi'an Jiaotong University. All the surgeries were performed under chloral hydrate anesthesia, and all efforts were made to minimize suffering.

Groups and treatments. All the animals were randomly assigned into three groups: Control (n=20), low selenium (LS) (n=20) and selenium supplementation (SS) (n=20). In the control group, the animals were fed with the standard diet for 14 weeks and were treated by intraperitoneal injection of physiological saline every day for 21 days. In the LS group, the animals were fed with the low-selenium diet for 14 weeks and were treated by intraperitoneal injection of physiological saline every day for 21 days. In the SS group, the animals were fed with the low-selenium diet for 14 weeks and were treated by intraperitoneal injection of sodium selenite (0.05 mg/kg bodyweight; Sigma-Aldrich, St. Louis, MO, USA) as selenium supplementation every day for 21 days (21). All the animals were monitored every two days by observing their mental status and activities. Two animals succumbed as a result of Se deficiency. Following this, these two animals were immediately quarantined and sent to the Animal Center for unified treatment.

Selenium concentration detection. Samples of whole blood and hearts harvested from rats were wet-washed by mixed acids (nitric acid and perchloric acid) in borosilicate reaction tubes. Following removal of the excess acids, the samples were titrated to 10 ml by ultra-pure water (Aqulix 5 water purification system; Merck Millipore, Billerica, MA, USA). The selenium concentration was subsequently determined by the flameless atomic absorption spectrophotometry method using a Z-5000 spectrophotometer (Hitachi, Ltd., Tokyo, Japan) with a cathode lamp of Se (resonance line, 196.0 nm; Photron, Victoria, Australia). Standard selenium solutions were used to calibrate the results.

Glutathione peroxidase activity assay. Cardiac glutathione peroxidase (GPx) activity in heart extract was assessed by a spectrophotometry method using the Glutathione Peroxidase Cellular Activity Assay kit (Sigma-Aldrich), following the manufacturer's instructions. The assay is based on the reaction in which oxidation of glutathione (GSH) to oxidized glutathione (GSSG) is catalyzed by GPx. As NADPH is consumed when GSSG is recycled back to GSH, the decrease in NADPH absorbance at 340 nm (Tecan Sunrise Absorbance Reader, Tecan, Austria) can be utilized to calculate the activity of GPx indirectly.

Plasma brain natriuretic peptide (BNP) assay. Following femoral artery puncture, whole blood samples were collected using EDTA-Na$_2$ vacuum blood collection tubes. The supernatant was collected after centrifugation at 377 x g for 20 min. The samples were processed by the Triage BNP assay (Biosite, San Diego, CA, USA) within 1 h after collection at room temperature, according to the manufacturer's instructions.

Electrocardiography (ECG). ECG in lead II was recorded (PowerLab 4/25; ADInstrument, New South Wales, Australia) during the experiment time. Prior to electrocardiography, all the rats were anesthetized by intraperitoneal injection of chloral hydrate (10%, 0.03 ml/kg bodyweight). The left upper limb, right upper limb and right lower limb electrodes were placed for leads I. Subsequently, the ECG was analyzed for changes in the ST segment, T wave, AV block and arrhythmia (premature ventricular contraction, ventricular tachycardia and fibrillation and atrial fibrillation). Cardiac conduction of rats was evaluated by the number of ventricular arrhythmic events (VAEs) within 15 min.

Echocardiography. Echocardiographic tests were performed according to the instructions described in previous studies (22,23). Animals were anesthetized with chloral hydrate (10%, 0.03 ml/kg bodyweight) intraperitoneally 10 min before imaging. In order to maintain an optimal image quality, the hair of the anterior chest wall was removed by 7% sodium sulfite solution and the rats were placed left laterally. Vivid 7 dimension (GE Healthcare, Pittsburgh, PA, USA) with a probe (12 L) working at 10 MHz was utilized. The probe was placed parallel to the left margin of the sternum and adjusting the image depth, ranging 2.0-4.0 cm. Regurgitant

jets were assessed by two-dimensional color and continuous Doppler. M-mode tracings were applied to determine the left ventricular end-systole diameter (LVESD) and left ventricular end-diastole diameter (LVEDD). Finally, the functional parameters, including left ventricular fractional shortening (LVFS%), which is the percentage of blood ejected by the left ventricle for each heart beat, and left ventricular ejection fraction (LVEF%), which measures the change in the left ventricular diameter from each diastole to systole were calculated respectively: LVFS% = ((LVEDD – LVESD)/LVEDD)%; and LVEF% = [(LVEDV – LVESV)/LVEDV]%.

Hemodynamic parameters. Hemodynamic determination was conducted according to methods described in a previous study (24). The animals were anesthetized with chloral hydrate (10%, 0.03 ml/kg bodyweight) intraperitoneally. A catheter connected to the Powerlab 4/25 biological analysis system was intubated from the right carotid artery into the left ventricle. Left ventricular systolic pressure (LVSP), left ventricular end-diastolic pressure (LVEDP), maximum rising rate of left ventricular pressure ($LVdp/dt_{max}$) and maximum dropping rate of left ventricular pressure ($LVdp/dt_{min}$) were measured.

Histological examination. The animals were anesthetized with chloral hydrate (10%, 0.03 ml/kg bodyweight) intraperitoneally. Subsequently, they were sacrificed by removing the hearts following complete anesthesia. The harvested hearts were rinsed in phosphate-buffered saline, fixed in 4% paraformaldehyde for 24 h, embedded in paraffin and cross-sectioned into 10-μm slices. The sections were stained with hematoxylin and eosin (HE) for cells alignment according to the general procedure. The morphological structures of the heart were observed by light microscopy.

miRNA microarray analysis. Total RNA was isolated using TRIzol (Invitrogen) and the miRNeasy mini kit (Qiagen) according to the manufacturer's instructions, which efficiently recovered all RNA species, including miRNAs. RNA quality and quantity was measured by using nanodrop spectrophotometer (ND-1000, Nanodrop Technologies, Wilmington, DE, USA) and RNA integrity was determined by gel electrophoresis. Following RNA isolation from the samples, the miRCURY™ Hy3™/Hy5™ Power labeling kit (Exiqon, Vedbaek, Denmark) was used according to the manufacturer's guideline for miRNA labeling. Each sample (1 μg) was 3'-end-labeled with the Hy3TM fluorescent label, using T4 RNA ligase as follows: RNA in 2.0 μl water was combined with 1.0 μl calf intestinal alkaline phosphatase (CIP) buffer and CIP (Exiqon). The mixture was incubated for 30 min at 37°C, and was terminated by incubation for 5 min at 95°C. Subsequently, 3.0 μl labeling buffer, 1.5 μl fluorescent label (Hy3TM), 2.0 μl dimethyl sulfoxide and 2.0 μl labeling enzyme were added into the mixture. The labeling reaction was incubated for 1 h at 16°C, and terminated by incubation for 15 min at 65°C. Subsequent to stopping the labeling procedure, the Hy3TM-labeled samples were hybridized on the miRCURYTM LNA Array (v.16.0) (Exiqon) according to the array instructions. The total mixture (25 μl) from Hy3TM-labeled samples with 25 μl hybridization buffer were first denatured for 2 min at 95°C, incubated on ice for 2 min and hybridized to the microarray for 16-20 h

at 56°C in a 12-Bay Hybridization System (Hybridization System-Nimblegen Systems, Inc., Madison, WI, USA), which provides an active mixing action and constant incubation temperature to improve hybridization uniformity and to enhance the signal. Following hybridization, the slides were obtained, washed several times using Wash buffer kit (Exiqon), and dried by centrifugation for 5 min at 100 x g. Subsequently, the slides were scanned using the Axon GenePix 4000B microarray scanner (Axon Instruments, Foster City, CA). The scanned images were imported into the GenePix Pro 6.0 software (Axon Instruments) for grid alignment and data extraction. Replicated miRNAs were averaged and miRNAs with intensities >50 in all the samples were chosen for calculating normalization factor. Expressed data were normalized using the Median normalization (25). Following normalization, differentially expressed miRNAs were identified through fold change filtering. Hierarchical clustering was performed using the MEV software (Dana-Farber Cancer Institute, Boston, MA, USA).

Gene ontology (GO) analysis. GO analysis was applied in order to organize genes into hierarchical categories and uncover the miR-gene regulatory network on the basis of biological process and molecular function. In detail, two-side Fisher's exact test was used to classify the GO category, and the false discovery rate (FDR) was calculated to correct the P-value. Only GOs that had a P-value of <0.001 and an FDR of <0.05 were chosen. Within the significant category, the enrichment rare earth (Re) was: $Re=(n_f/n)/(N_f/N)$, where n_f is the number of flagged genes within the particular category, n is the total number of genes within the same category, N_f is the number of flagged genes in the entire microarray and N is the total number of genes in the microarray. Subsequently, the apoptosis-related network of miRNA-mRNA interaction, representing the critical miRNAs and their targets, was established according to the degree of miRNA (26).

Reverse transcription-quantitative polymerase chain reaction (RT-qPCR) of miRNA. Differentially expressed miRNAs of *miR-374*, *miR-16*, *miR-199a-5p*, *miR-195*, *miR-30e**, *miR-3571*, *miR-675* and *miR-450a** were selected for verification. Total RNA was extracted from harvested heart using the MiniBEST Universal RNA Extraction kit (Takara, Otsu, Japan). cDNA was synthesized from total RNA with the SYBR PrimeScript™ miRNA RT-PCR kit (Takara). The expression of miRNA was analyzed by qPCR using SYBR Premix Ex TaqTMII (Takara). PCR was performed in triplicate for each sample. The relative amount of miRNAs was normalized against *U6* small nuclear RNA. Detection of mRNA was performed as described previously (27). The sequences of the primers are shown in Table I.

Western blotting. Frozen cardiac tissue was homogenized in radioimmunoprecipitation assay lysis buffer system (Santa Cruz Biotechnology, Inc., Dallax, TX, USA) with phenylmethylsulfonyl fluoride (Santa Cruz Biotechnology, Inc.). All the procedures followed manufacturer's instructions. The sample protein concentration was detected by using bicinchoninic acid protein assay kit (Santa Cruz Biotechnology, Inc.). The sample protein was boiled in 1x SDS-PAGE loading buffer, separated by electrophoresis in 10% SDS-polyacrylamide gel and subsequently transferred to a polyvinylidene fluoride membrane.

Table I. Primers used in TaqMan RT-qPCR.

Gene primer	Product size, bp	Number gene primer (5'→3')
U6	62	F: 5'-GCTTCGGCAGCACATATACTAAAAT-3'
		R: 5'-CGCTTCACGAATTTGCGTGTCAT-3'
rno-miR-374	68	F: 5'-CTCGGATGGATATAATACA-3'
		R: 5'-CTCGGACAATAATAATACA-3'
rno-miR-16	62	F: 5'-GGGGTAGCAGCACGTAAATA-3'
		R: 5'-GTGCGTGTCGTGGAGTCG-3'
rno-miR-199a-5p	94	F: 5'-CTTCTGGAGATCCTGCTC-3'
		R: 5'-TGCCCAGTCTAACCAATG-3'
rno-miR-195	78	F: 5'-AACTCTCCTGGCTCTAGC-3'
		R: 5'-GCCTGGAGCAGCACAG-3'
rno-miR-30e	86	F: 5'-GGGCAGTCTTTGCTACTG-3'
		R: 5'-CCTGCCGCTGTAAACATC-3'
rno-miR-3571	96	F: 5'-GGACATTACCTACCCAA-3'
		R: 5'-TAGTGCCTACTCAGAGC-3'
rno-miR-675	70	F: 5'-GGACTGGTGCGGAAAGG-3'
		R: 5'-AGACCCAGGGACTGAGC-3'
rno-miR-450a	70	F: 5'-AGAGATGCGGAGCTGTT-3'
		R: 5'-TATGCAAAATGTTCCCAAT-3'

RT-qPCR, reverse transcription-quantitative polymerase chain reaction; bp, base pair; F, forward primer; R, reverse primer.

Antibodies against Wnt (ab15251) and β-catenin (ab6302) (Abcam, Cambridge, MA, USA) were applied to incubate the bolts at 4°C overnight. Tris-buffered saline (containing 0.02% Tween 20) was used to wash the membranes, which were subsequently incubated with goat polyclonal secondary antibody to rabbit immunoglobulin G conjugated to horseradish peroxidase (Abcam). The membranes were developed using Super Signal West Pico chemiluminescence reagent (Thermo Scientific, Waltham, MA, USA) and were visualized on X-ray films.

Statistical analysis. All the results were expressed as mean ± standard deviation. Statistical analysis was performed with one-way analysis of variance for multiple comparisons. $P<0.05$ was considered to indicate a statistically significant difference.

Results

Se concentration in blood samples. The Se concentration in blood is shown in Fig. 1. Significant changes of Se concentration were observed in the LS and SS groups. Compared to the control group, the Se concentration in blood decreased significantly in the LS and SS groups ($P<0.05$). Se intraperitoneal injection was proved to increase the Se concentration in blood in the SS group compared to the LS group ($P<0.05$).

Effects of Se deficiency and Se supplementation on GPx activity. As shown in Fig. 2, the activity of GPx in the LS and SS groups decreased significantly compared to the control group ($P<0.05$). The activity of GPx was observed to reduce more significantly in the LS group. However, an evident recovery of GPx activity in the SS group was confirmed by the GPx activity assay when compared to the LS group ($P<0.05$).
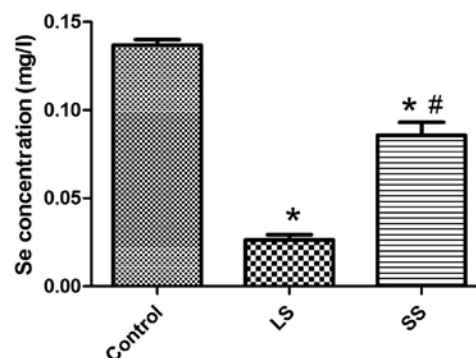

Figure 1. Se concentrations for each group. Se concentrations in the blood of rats were analyzed by spectrophotometry. *$P<0.05$ vs. control; #$P<0.05$ vs. LS. LS, low selenium; SS, selenium supplementation.
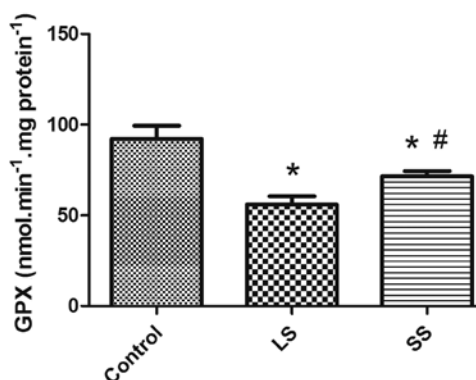

Figure 2. Effects of Se deficiency/supplementation on GPx activity. A spectrophotometry method was utilized to examine the activity of GPx. Values indicated by columns in the graph are presented as mean ± standard deviation. *$P<0.05$ vs. control; #$P<0.05$ vs. LS. LS, low selenium; SS, selenium supplementation; GPx, glutathione peroxidase.

Table II. Echocardiographic parameters of the rats in the different groups.

Group	No.	LVEDD, mm	LVESD, mm	LVEF, %	LVFS, %
Control	10	4.14±0.38	1.13±0.77	85.60±11.02	75.64±8.30
LS	10	5.29±0.26[a*]	2.77±0.35[a,c]	68.93±10.92[a,c]	50.44±5.73[a,d]
SS	10	4.92±0.79[b*]	2.05±0.23[b,c]	79.20±9.41[b,c]	97.73±6.28[b,d]

Cardiac functions (left ventricular functions) were assessed by echocardiographic detection. All the results are presented as mean ± standard deviation. [a]Values are significantly different from the control (P<0.05) ([c]P<0.05; [d]P<0.01). [b]Values are significantly different from the LS group (P<0.05) ([c]P<0.05; [d]P<0.01). LVEDD, left ventricular end-diastole diameter; LVESD, left ventricular end-systole diameter; LVEF, left ventricular ejection fraction; LVFS, left ventricular fractional shortening.

Plasma BNP. The Triage BNP assay showed that the plasma BNP level increased significantly in the LS and SS groups compared to the control group (P<0.05). A clearer increase of plasma BNP was found in the LS group. Following Se supplementation by intra-peritoneal injections, a reduction in the plasma BNP level in the SS group was identified compared to the LS group (P<0.05) (Fig. 3).

ECG features. ECG of rats in the control group was normal (Fig. 4A). However, ECG of rats in the LS group showed significant differences. In the LS group, a few rats exhibited normal ECG, but the majority had abnormal ECG, which manifested as premature ventricular contraction and paroxysmal supraventricular tachycardia (Fig. 4B and C). The majority of ECG in the SS group were normal, but there remained a few abnormal ECG (Fig. 4D). VAEs in the LS group were higher than those of the control group (P<0.05), but following Se supplementation the VAEs significantly decreased compared to the LS group (P<0.05) (Fig. 4E).

Echocardiographic detection. The echocardiographic parameters, including LVEDD, LVESD, LVEF and LVFS, were detected and calculated in the present study as shown in Table II. An overall increase of LVEDD and LVESD accompanied by an overall decrease of LVEF and LVFS were found in the LS and SS groups. However, there was a significant increase of LVEDD and LVESD and a significant decrease of LVEF and LVFS in the LS group compared to the SS group. A significant recovery of cardiac function marked by echocardiographic parameters was found in the SS group compared to the LS group, which was evidenced by restoration of LVEDD, LVESD, LVEF and LVFS following Se supplementation.

Hemodynamic detection. The hemodynamic parameters, including LVEDP, LVSP, LVdp/dt$_{max}$ and LVdp/dt$_{min}$, were detected and calculated in the study as shown in Table III. An overall increase of LVEDP and LVSP accompanied by an overall decrease of LVdp/dt$_{max}$ and LVdp/dt$_{min}$ were found in the LS and SS groups. However, there was a significant increase of LVEDP and LVSP and decrease of LVdp/dt$_{max}$ and LVdp/dt$_{min}$ in the LS group compared to the SS group. A significant recovery of cardiac function marked by hemodynamic parameters was found in the SS group compared to the LS group, which was evidenced by restoration of LVEDP, LVSP, LVdp/dt$_{max}$ and LVdp/dt$_{min}$ following Se supplementation.
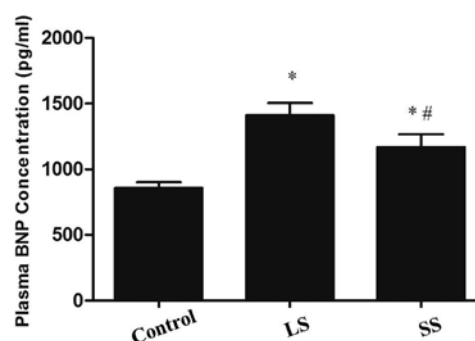

Figure 3. Effects of Se deficiency/supplementation on plasma BNP level. Plasma BNP concentration (pg/ml) was examined by the Triage BNP Assay. The values indicated by the columns in the graph are presented as mean ± standard deviation. *P<0.05 vs. control; #P<0.05 vs. LS. LS, low selenium; SS, selenium supplementation; BNP, brain natriuretic peptide.

Histological characterization of the heart. HE staining showed that the structure of myocardial tissue in the control group was clear, including well-connected intercalated discs and normally arranged filaments (Fig. 5A). In the LS group, the muscle fibers of the rats were swelling and disorganized (Fig. 5B). Myocardial necrosis, nuclear condensation and partially intermittent muscle fibers were observed in the LS group (Fig. 5C and D). In addition, the small myocardial necrosis focus accompanied by inflammatory infiltration can be observed in certain areas (Fig. 5E). Following Se supplementation, the myocardial fibers were mildly swelling compared to the control group, but their arrangements were orderly (Fig. 5F).

miRNA expression profiles. Using the miRCURY LNA Array platform, the miRNAs expression profiles were assessed in Se-deficient rats. The expression profiles of 116 miRNAs were regulated between the control, LS and SS groups, and the samples were separated into biologically interpretable groups. Among these, 5 miRNAs were identified to be upregulated >5-fold in the LS group compared to the SS group, whereas 3 miRNAs were less than the threshold level (3-fold) set during the progression of Se deficiency, but following selenium supplementation these miRNAs were >1.5-fold compared to Se deficiency. These 8 miRNAs were validated to be significantly different (P<0.05). As shown in Fig. 6, the levels of *miR-374*, *miR-16*, *miR-199a-5p*, *miR-195* and *miR-30e*[*] were upregulated in rats with selenium deficiency,

Table III. Hemodynamic parameters of the rats in the different groups.

Group	No.	LVEDP, mmHg	LVSP, mmHg	LVdp/dt$_{max}$, mmHg/sec	LVdp/dt$_{min}$, mmHg/sec
Control	7	47.62±6.41	185.32±13.28	3794.55±127.47	2887.65±154.13
LS	8	67.81±5.50[a]*	157.69±14.24[a,c]	2640.31±144.20[a,c]	2216.28±138.69[a,c]
SS	8	53.29±5.13[b]**	162.30±14.68[b,c]	2948.19±152.35[b,c]	2677.00±142.98[b,c]

Cardiac functions (left ventricular functions) were assessed by hemodynamic tests using a cardiac intubation method. All the results are presented as mean ± standard deviation. [a]Values are significantly different from the control ([c]$P<0.05$). [b]Values are significantly different from the LS group ([c]$P<0.05$). LS, low selenium; SS, selenium supplementation; LVSP, left ventricular systolic pressure; LVEDP, left ventricular end-diastole pressure; LVdp/dt$_{max}$, maximum rising rate of left ventricular pressure; LVdp/dtmin, maximum dropping rate of left ventricular pressure.
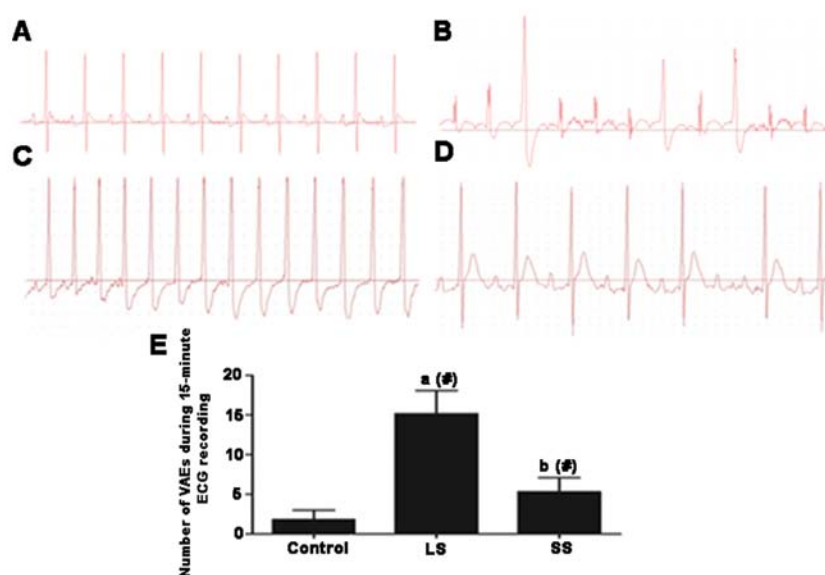

Figure 4. ECG features. (A) Normal ECG in the control group, (B) premature ventricular contraction in the LS group, (C) paroxysmal supraventricular tachycardia in the LS group and (D) premature atrial contraction in the SS group. (E) Analysis of VAEs ([a,#]$P<0.001$ vs. control; [b,#]$P<0.001$ vs. LS). ECG, electrocardiography; LS, low selenium; SS, selenium supplementation; VAE, ventricular arrhythmic event.
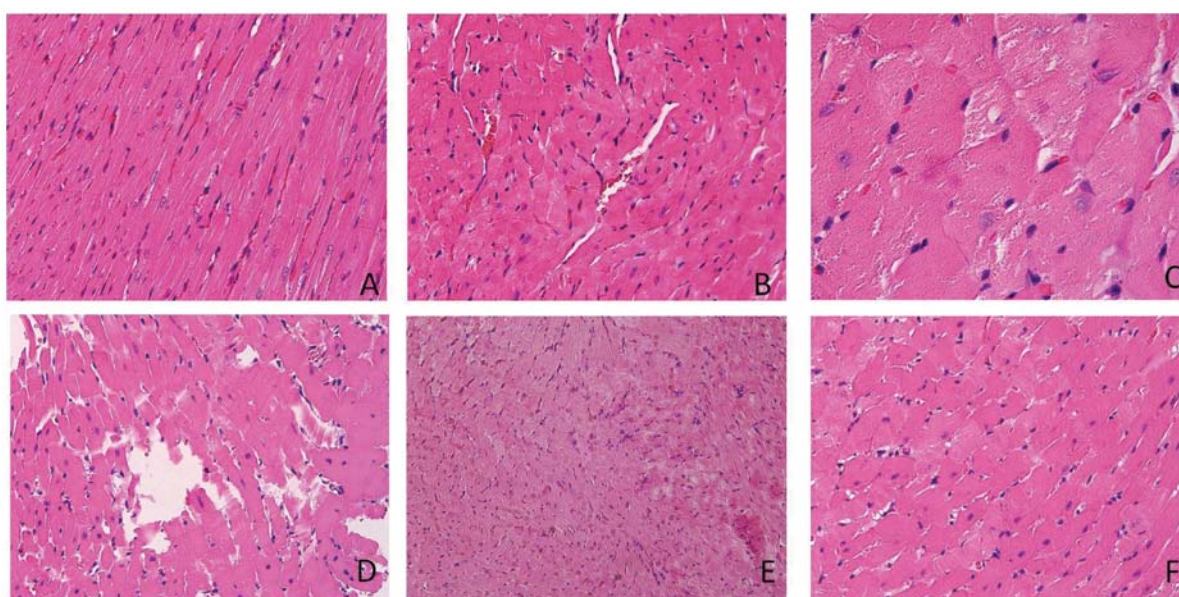

Figure 5. Histological changes of the rat hearts. (A) Control, (B-E) LS and (F) SS groups. (A) Normal structure of myocardial tissue (magnification: x400). (B) Swelling hend disorganized muscle fibers (magnification, x400). (C) Myocardial necrosis and nuclear condensation (magnification, x1000). (D) Intermittent muscle fibers (magnification, x400). (E) Small myocardial necrosis stove accompanied by inflammatory infiltration (magnification, x200). (F) Mild swelling and orderly arrangement myocardial fibers (magnification, x400). LS, low selenium; SS, selenium supplementation.
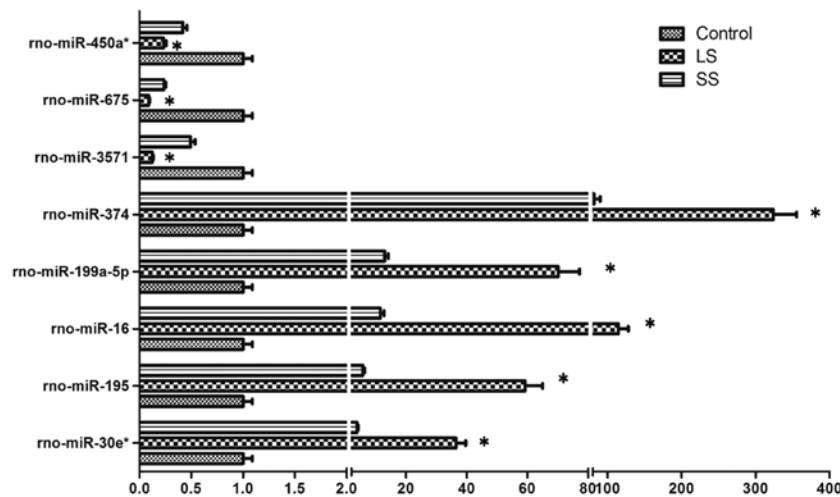
Figure 6. miRNA profiles differentiate rats with normal diet from rats with Se deficiency or Se supplementation. Five upregulated (*miR-374*, *miR-16*, *miR-199a-5p*, *miR-195* and *miR-30e**) and three downregulated (*miR-3571*, *miR-675* and *miR-450a**) miRNAs were identified using RT-qPCR. Triplicate assays were performed for each RNA sample and the relative amount of each miRNA was normalized to *U6* smal nuclear RNA. A statistically significant difference between every group is indicated by *P<0.01. LS, low selenium; SS, selenium supplementation; RT-qPCR, reverse transcription-quantitative polymerase chain reaction.
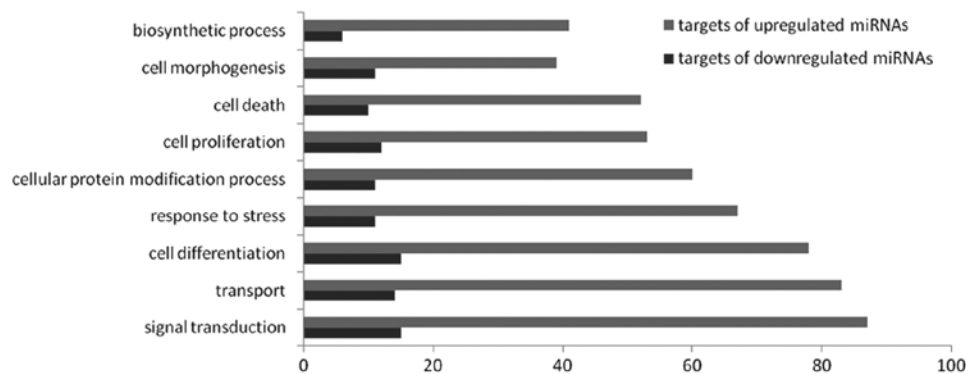

Figure 7. GO of significant microRNAs. The gray column shows the GOs targeted by upregulated miRNAs and the black column shows the GOs targeted by downregulated miRNAs. All these GOs show increased enrichment. The vertical axis is the GO category and the horizontal axis is the enrichment of GO. GO, gene ontology.

while *miR-3571*, *miR-675* and *miR-450a** showed an opposite expression pattern, in agreement with the results of micro-array hybridization.

Microarray-based GO analysis. According to the threshold of GOs that were significantly regulated by miRNAs, the P-value and FDR was <0.001 and <0.05, respectively. The high-enrichment GOs targeted by upregulated miRNAs included signal transduction, transport, cell differentiation and response to stress. By contrast, the significant GOs corresponding to downregulated miRNAs appeared to include signal transduction, cell differentiation, transport and cell proliferation. Among these, the maximum-enriched-GO associated with signal transduction, together with the numerous miRNAs that interacted with signal transduction-related genes, suggested them to have an important role in the activation of selenium deficiency (Fig. 7).

Expression of Wnt/β-catenin. Western blotting was employed to detect the changes of Wnt and β-catenin expression in the present study. As shown in Fig. 8, the protein expression of Wnt and β-catenin in cardiac tissue were highest in the LS group compared to the control group. Increasing expression of Wnt and β-catenin in the LS group was decreased by Se supplementation. However, it appeared that Se supplementation reversed the increasing expression of Wnt and β-catenin in the LS group.

Discussion

In China, KD is the most detrimental and widely distributed endemic cardiomyopathy. In an observational epidemiological study and from population-based intervention trial results, it was concluded that Se deficiency is the critical etiological factor for KD (28-31). An early population-based clinical study showed that a low selenium level was associated with cardiovascular outcomes (32). In a recent prospective cohort study of patients with coronary artery disease, the individual baseline serum selenium concentration was inversely associated with mortality of acute coronary syndrome. Low serum
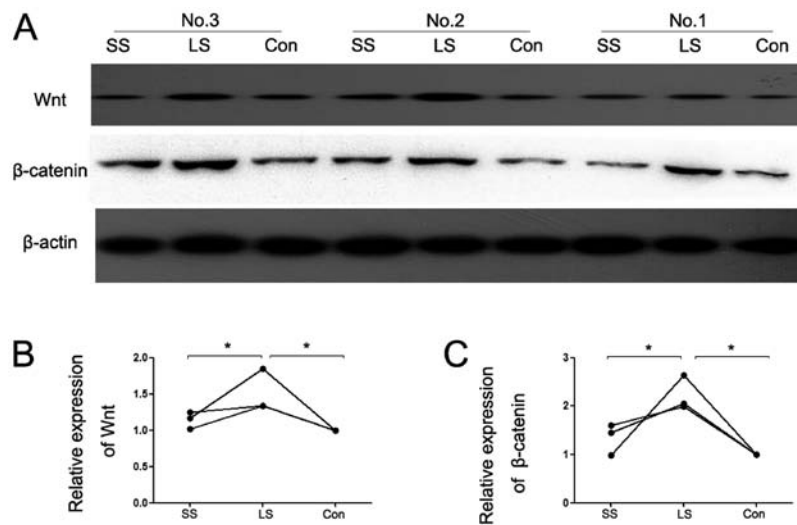
Figure 8. Effects of Se deficiency and Se supplementation on protein expression of Wnt and β-catenin in cardiac tissue. Sample protein was extracted, separated and detected by specific antibodies against Wnt and β-catenin. The expression of Wnt and β-catenin were normalized by β-actin in the same sample. The darkness of the immunoblots represents the expression level of the protein. (A) Western blotting of Wnt and β-catenin. (B) Analysis of the relative expression of Wnt and (C) β-catenin normalized by β-actin. *Values are significantly different from LS (P<0.05). LS, low selenium; SS, selenium supplementation.

selenium was considered independent of classic risk factors, including biomarkers of necrosis and LVEF, of acute coronary syndrome (33). In an animal study, Se deficiency was associated with evident worsening of cardiac functional parameters and cardiac hypertrophy, associated with a marked decrease of GPx activity in cardiac tissue (34). In the present study, the deterioration of cardiac function in rats receiving a low-Se diet by plasma BNP and echocardiographic determinations was determined. The results demonstrated that the serum BNP level, LVEDD and LVESD increased, and LVEF and LVFS decreased in low-Se-diet treated rats. These results were in accordance with those in the above studies.

Increasing evidence has confirmed miRNA as one of the most significant and critical factors controlling gene expression. Thus far, miRNAs have been noted to play an extremely important role in cardiac development, homeostasis and pathobiology (35,36). Although miRNAs function as endogenous intracellular regulators of mRNA translation, they can be detected in circulating blood or its components in a markedly stable form and, therefore, should be considered as disease biomarkers, for instance, in cardiovascular diseases (37,38). A series of significant advances have been found in the research of cardiac hypertrophy (39), congenital heart disease (40), heart failure (41,42), arrhythmia (43), arterial atherosclerosis (44) and hypertension (45), and miRNAs have become a current interest for international cardiovascular research. However, no research has been reported regarding miRNAs and KD thus far. Therefore, the miRNAs expression profile in rats with Se deficiency was evaluated. In comparison to those of Se supplementation and normal Se supply, the microarray revealed a set of differentially expressed miRNAs, 5 significantly upregulated and 3 significantly downregulated, in the rats with Se deficiency. Evaluation of *miR-374*, *miR-16*, *miR-199a-5p*, *miR-195*, *miR-30e*, *miR-3571*, *miR-675* and *miR-450a* further validated the reliability of micoarray hybridization.

Molecular mechanisms underlying cardiac dysfunction caused by Se deficiency should be intensively studied. Wnt signaling is required for various features of cardiac and vascular development, such as myocardial specification, cardiac morphogenesis and cardiac valve formation, as well as endothelial and vascular smooth muscle cell proliferation (46). Defective Wnt signaling can lead to various cardiac and vascular abnormalities. Wnt signaling activity is quite low under normal conditions in the adult heart and blood vessels. However, during the pathological cardiac remodeling induced by pressure overload, in injured arteries and following myocardial infarction, this pathway is reactivated. Genetically modified animal models have shown that inhibition of Wnt signaling results in increased angiogenesis, improved infarct healing and an attenuated hypertrophic response of the heart, indicating that pharmacological inhibition of Wnt signaling provided a novel therapeutic strategy to prevent excessive cardiac and vascular remodeling (47). The β-catenin gene is a critical component of the Wnt signaling, where it transmits extracellular Wnt signals to the nucleus. The level of β-catenin in the cytoplasm and nucleus is tightly regulated. In the absence of the Wnt signal, cytoplasmic β-catenin is maintained at a low level through ubiquitin-mediated proteasomal degradation, which is controlled by the destruction complex consisting of glycogen synthase kinase 3b/adenomatous polyposis coli/Axin. Upon receiving Wnt signals, cell degradation of β-catenin by the destruction complex and ubiquitin-proteasome complex is inhibited, resulting in accumulation of β-catenin in the cytoplasm and translocation into the nucleus. β-catenin heterodimerizes with members of the TCF/LEF transcription factors to activate transcription of the target genes in the nucleus. The nuclear translocation of β-catenin is involved in epithelial-mesenchymal transformation, which is an initial and critical step in fibrosing processes, including pulmonary fibrosis and myocardial infarction repair (48,49). Zelarayán *et al* (50) found that β-catenin depletion was beneficial in postinfarction LV remodeling partly through enhanced differentiation of α-MHC[pos] cardiac resident progenitor cells. Downregulation of β-catenin improved cardiac function

following experimental infarction. The study indicated that endogenous cardiac regeneration contributes to LV remodeling following chronic ischemia through differentiation of resident precursor cells, amplified by β-catenin downregulation (50). In the present study, selenium deficiency was demonstrated to result in cardiac dysfunction by increasing the expression of Wnt and β-catenin, however, following selenium supplementation cardiac function partially recovery and Wnt and β-catenin expression decreased compared to the LS group. Therefore, the Wnt/β-catenin signaling pathway may be involved in the process of cardiac function deterioration.

In conclusion, Se deficiency is associated with eight miRNAs: *miR-374, miR-16, miR-199a-5p, miR-195, miR-30e*, miR-3571, miR-675* and *miR-450a**. Their wide range of actions may regulate cardiac function. The expression of *miR-374* was the highest, which may be significant in rats with selenium deficiency. The possible mechanism of cardiac dysfunction was associated with the Wnt/β-catenin signaling pathway. These findings not only highlight the incidence of cardiac dysfunction caused by Se deficiency, but also facilitate access to a novel therapeutic strategy from a molecular level against cardiac dysfunction and offer insight into its progression.

Acknowledgements

References

1. Ge K, Xue A, Bai J and Wang S: Keshan disease-an endemic cardiomyopathy in China. Virchows Arch A Pathol Anat Histopathol 401: 1-15, 1983.
2. Oster O, Prellwitz W, Kasper W and Meinertz T: Congestive cardiomyopathy and the selenium content of serum. Clin Chim Acta 128: 125-132, 1983.
3. de Lorgeril M, Salen P, Accominotti M, Cadau M, Steghens JP, Boucher F and de Leiris J: Dietary and blood antioxidants in patients with chronic heart failure. Insights into the potential importance of selenium in heart failure. Eur J Heart Fail 3: 661-669, 2001.
4. Arroyo M, Laguardia SP, Bhattacharya SP, Nelson MD, Johnson PL, Carbone LD, et al: Micronutrients in African-Americans with decompensated and compensated heart failure. Transl Res 148: 301-308, 2006.
5. Witte KK, Nikitin NP, Parker AC, von Haehling S, Volk HD, Anker SD, et al: The effect of micronutrient supplementation on quality-of-life and left ventricular function in elderly patients with chronic heart failure. Eur Heart J 26: 2238-2244, 2005.
6. Djuranovic S, Nahvi A and Green R: A parsimonious model for gene regulation by miRNAs. Science 331: 550-553, 2011.
7. Ambros V: The functions of animal microRNAs. Nature 431: 350-355, 2004.
8. Viader A, Chang LW, Fahrner T, Nagarajan R and Milbrandt J: MicroRNAs modulate Schwann cell response to nerve injury by reinforcing transcriptional silencing of dedifferentiation-related genes. J Neurosci 31: 17358-17369, 2011.
9. Roldo C, Missiaglia E, Hagan JP, Falconi M, Capelli P, Bersani S, et al: MicroRNA expression abnormalities in pancreatic endocrine and acinar tumors are associated with distinctive pathologic features and clinical behavior. J Clin Oncol 24: 4677-4684, 2006.
10. Zhao JJ, Hua YJ, Sun DG, Meng XX, Xiao HS and Ma X: Genome-wide microRNA profiling in human fetal nervous tissues by oligonucleotide microarray. Childs Nerv Syst 22: 1419-1425, 2006.
11. Bhanot P, Brink M, Samos CH, Hsieh JC, Wang Y, Macke JP, et al: A new member of the frizzled family from Drosophila functions as a Wingless receptor. Nature 382: 225-230, 1996.
12. Tamai K, Semenov M, Kato Y, Spokony R, Liu C, Katsuyama Y, et al: LDL-receptor-related proteins in Wnt signal transduction. Nature 407: 530-535, 2000.
13. Kishida S, Yamamoto H, Ikeda S, Kishida M, Sakamoto I, Koyama S and Kikuchi A: Axin, a negative regulator of the wnt signaling pathway, directly interacts with adenomatous polyposis coli and regulates the stabilization of beta-catenin. J Biol Chem 273: 10823-10826, 1998.
14. Sakanaka C, Weiss JB and Williams LT: Bridging of beta-catenin and glycogen synthase kinase-3beta by axin and inhibition of beta-catenin-mediated transcription. Proc Natl Acad Sci USA 95: 3020-3023, 1998.
15. Behrens J, Jerchow BA, Wurtele M, Grimm J, Asbrand C, Wirtz R, et al: Functional interaction of an axin homolog, conductin, with beta-catenin, APC, and GSK3beta. Science 280: 596-599, 1998.
16. Kawano Y and Kypta R: Secreted antagonists of the Wnt signalling pathway. J Cell Sci 116: 2627-2634, 2003.
17. Cadigan KM: Wnt-beta-catenin signaling. Curr Biol 18: R943-R947, 2008.
18. Rao TP and Kuhl M: An updated overview on Wnt signaling pathways: a prelude for more. Circ Res 106: 1798-1806, 2010.
19. Klaus A and Birchmeier W: Wnt signalling and its impact on development and cancer. Nat Rev Cancer 8: 387-398, 2008.
20. Katoh M and Katoh M: Wnt signaling pathway and stem cell signaling network. Clin Cancer Res 13: 4042-4045, 2007.
21. Dursun N, Taskin E, Yerer AM and Sahin L: Selenium-mediated cardioprotection against adriamycin-induced mitochondrial damage. Drug Chem Toxicol 34: 199-207, 2011.
22. Gu L, Pandey V, Geenen DL, Chowdhury SA and Piano MR: Cigarette smoke-induced left ventricular remodelling is associated with activation of mitogen-activated protein kinases. Eur J Heart Fail 10: 1057-1064, 2008.
23. Ma J, Qian J, Ge J, Zeng X, Sun A, Chang S, et al: Changes in left ventricular ejection fraction and coronary flow reserve after coronary microembolization. Arch Med Sci 8: 63-69, 2012.
24. Jiang K, Shui Q, Xia Z and Yu Z: Changes in the gene and protein expression of K (ATP) channel subunits in the hippocampus of rats subjected to picrotoxin-induced kindling. Brain Res Mol Brain Res 128: 83-89, 2004.
25. Zhang L, Yang M, Marks P, White LM, Hurtig M, Mi QS, Divine G and Gibson G: Serum non-coding RNAs as biomarkers for osteoarthritis progression after ACL injury. Osteoarthritis Cartilage 20: 1631-1637, 2012.
26. Guo CJ, Pan Q, Li DG, Sun H and Liu BW: miR-15b and miR-16 are implicated in activation of the rat hepatic stellate cell: An essential role for apoptosis. J Hepatol 50: 766-778, 2009.
27. Guan H, Song L, Cai J, Huang Y, Wu J, Yuan J, et al: Sphingosine kinase 1 regulates the Akt/FOXO3a/Bim pathway and contributes to apoptosis resistance in glioma cells. PLoS One 6: e19946, 2011.
28. Chen J: An original discovery: selenium deficiency and Keshan disease (an endemic heart disease). Asia Pacific J Clin Nutr 21: 320-326, 2012.
29. Xu GL: The effectiveness of sodium Selenite on prevention of acute attacks of Keshan diseases. Chin Med J 92: 471-476, 1979.
30. Chen X, Yang G, Chen J, Chen X, Wen Z and Ge K: Studies on the relationships of selenium and Keshan disease. Biol Trace Elem Res 2: 91-107, 1980.
31. Li Q, Liu M, Hou J, Jiang C, Li S and Wang T: The prevalence of Keshan disease in China. Int J Cardiol 168: 1121-1126, 2013.
32. Salonen JT, Alfthan G, Huttunen JK, Pikkarainen J and Puska P: Association between cardiovascular death and myocardial infarction and serum selenium in a matched-pair longitudinal study. Lancet 2: 175-179, 1982.
33. Lubos E, Sinning CR, Schnabel RB, Wild PS, Zeller T, Rupprecht HJ, et al: Serum selenium and prognosis in cardiovascular disease: results from the AtheroGene study. Atherosclerosis 209: 271-277, 2010.
34. Lymbury RS, Marino MJ and Perkins AV: Effect of dietary selenium on the progression of heart failure in the ageing spontaneously hypertensive rat. Mol Nutr Food Res 54: 1436-1444, 2010.
35. Latronico MV and Condorelli G: MicroRNAs and cardiac pathology. Nat Rev Cardiol 6: 419-429, 2009.
36. Porrello ER: microRNAs in cardiac development and regeneration. Clin Sci (Lond) 125: 151-166, 2013.
37. Van Aelst LN and Heymans S: MicroRNAs as biomarkers for ischemic heart disease. J Cardiovasc Transl Res 6: 458-470, 2013.
38. Nabialek E, Wanha W, Kula D, Jadczyk T, Krajewska M, Kowalowka A, et al: Circulating microRNAs (miR-423-5p, miR-208a and miR-1) in acute myocardial infarction and stable coronary heart disease. Minerva Cardioangiol 61: 627-637, 2013.

39. Sayed D, Hong C, Chen IY, Lypowy J and Abdellatif M: MicroRNAs play an essential role in the development of cardiac hypertrophy. Circ Res 100: 416-424, 2007.
40. Xing HJ, Li YJ, Ma QM, Wang AM, Wang JL, Sun M, *et al*: Identification of microRNAs present in congenital heart disease associated copy number variants. Eur Rev Med Pharmacol Sci 17: 2114-2120, 2013.
41. Melman YF, Shah R and Das S: MicroRNAs in heart failure: is the picture becoming less miRky? Circ Heart Fail 7: 203-214, 2014.
42. Oliveira-Carvalho V, Da SM, Guimaraes GV, Bacal F and Bocchi EA: MicroRNAs: new players in heart failure. Mol Biol Rep 40: 2663-2670, 2013.
43. Kim GH: MicroRNA regulation of cardiac conduction and arrhythmias. Transl Res 161: 381-392, 2013.
44. Madrigal-Matute J, Rotllan N, Aranda JF and Fernández-Hernando C: MicroRNAs and atherosclerosis. Curr Atheroscler Rep 15: 322, 2013.
45. Kontaraki JE, Marketou ME, Zacharis EA, Parthenakis FI and Vardas PE: Differential expression of vascular smooth muscle-modulating microRNAs in human peripheral blood mononuclear cells: novel targets in essential hypertension. J Hum Hypertens 28: 5410-516, 2014.
46. Gessert S and Kühl M: The multiple phases and faces of wnt signaling during cardiac differentiation and development. Circ Res 107: 186-199, 2010.
47. van de Schans VA, Smits JF and Blankesteijn WM: The Wnt/frizzled pathway in cardiovascular development and disease: friend or foe? Eur J Pharmacol 585: 338-345, 2008.
48. Blankesteijn WM, van Gijn ME, Essers-Janssen YP, Daemen MJ and Smits JF: Beta-catenin, an inducer of uncontrolled cell proliferation and migration in malignancies, is localized in the cytoplasm of vascular endothelium during neovascularization after myocardial infarction. Am J Pathol 157: 877-883, 2000.
49. Chilosi M, Poletti V, Zamò A, Lestani M, Montagna L, Piccoli P, *et al*: Aberrant Wnt/beta-catenin pathway activation in idiopathic pulmonary fibrosis. Am J Pathol 162: 1495-1502, 2003.
50. Zelarayán LC, Noack C, Sekkali B, Kmecova J, Gehrke C, Renger A, *et al*: Beta-Catenin downregulation attenuates ischemic cardiac remodeling through enhanced resident precursor cell differentiation. Proc Natl Acad Sci USA 105: 19762-19767, 2008.